Neurobiology of Aging 34 (2013) 1069–1079

Contents lists available at SciVerse ScienceDirect

Neurobiology of Aging

journal homepage: www.elsevier.com/locate/neuaging

Oxidative stress induces DNA demethylation and histone acetylation in SH-SY5Y cells: potential epigenetic mechanisms in gene transcription in Aβ production

Xinling Gu [1], Jing Sun [1], Shen Li, Xiangmei Wu, Liang Li*

Department of Pathology, Key Laboratory for Neurodegenerative Disease of Education Ministry, Capital Medical University, Beijing, China

ARTICLE INFO

Article history:
Received 29 June 2012
Received in revised form 10 October 2012
Accepted 16 October 2012
Available online 8 November 2012

Keywords:
Alzheimer's disease
Oxidative stress
Amyloid-β
DNA methylation
Histone acetylation
Nuclear factor-κB
Specific protein-1
SH-SY5Y cell

ABSTRACT

Overwhelming evidence has suggested that enhanced oxidative stress is involved in the pathogenesis and/or progression of Alzheimer's disease (AD). Amyloid-β (Aβ) that composes senile plaques plays a causal role in AD, and its abnormal deposition in brains is the typical neuropathologic hallmark of AD. Recent studies have suggested that epigenetic mechanisms play an important role in the initiation and development of AD. In the present study, we investigated the epigenetic mechanisms, such as DNA methylation and histone acetylation, involved in the transcription of AD-related genes with Aβ production under oxidative stress. Human neuroblastoma SH-SY5Y cells were treated with hydrogen peroxide (H_2O_2) and used as the cell model. The intracellular Aβ level was significantly increased in H_2O_2-treated SH-SY5Y cells. The expression of amyloid-β precursor protein and β-site amyloid-β precursor protein-cleaving enzyme 1 was upregulated by demethylation in the gene promoters associated with the reduction of methyltransferases. Meanwhile, H_2O_2 induced the upregulation of histone acetyltransferases p300/cAMP-response element binding protein (p300/CBP) and down-regulation of histone deacetylases. DNA hypomethylation induced by DNA methyltransferase inhibitor could activate the DNA binding activity of transcription factor nuclear factor-κB, whereas no significant effect was observed on specific protein 1. DNA binding activities of nuclear factor-κB and specific protein 1 were activated by histone hyperacetylation induced by histone deacetylase inhibitor. These findings suggested that oxidative stress resulted in an imbalance between DNA methylation and demethylation and histone acetylation and deacetylation associated with the activation of transcription factors, leading to the AD-related gene transcription in the Aβ overproduction. This could be a potential mechanism for oxidative stress response, which might contribute to the pathogenesis and development of AD.

1. Introduction

Alzheimer disease (AD) is defined as progressively impaired memory and cognition, and it is also characterized by the presence of extracellular neuritic plaques and intracellular neurofibrillary tangles. Altered proteolytic processing of the amyloid precursor protein (APP) plays a crucial role in the AD development, resulting in the overproduction and aggregation of neurotoxic forms of amyloid-β (Aβ) peptide. It has been postulated that different soluble or insoluble higher molecular weight forms of Aβ trigger a complex pathologic cascade that might cause synaptic dysfunction, inflammatory processes, neuronal loss, cognitive impairment, and finally the onset of the disease. An aspartyl protease (β-site APP-cleaving enzyme 1 [BACE1]) mediates the proteolytic cleavage of APP, which is a required process for Aβ generation. Most AD cases are sporadic and have no defined causes. Factors contributing to AD development are numerous and complex. In the last decade, overwhelming evidence has suggested that oxidative stress is exponentially increased with age through variations in the generation of reactive oxygen species (ROS), ROS elimination, or both (Barja, 2004). Oxidative stress is an early event in AD. It has been demonstrated that the early involvement of oxidative stress in AD includes oxidative modifications of lipids (Sayre et al., 1997; Schuessel et al., 2005), proteins (Montine et al., 1996; Smith et al., 1991), and nucleic acids (Nunomura et al., 2004, 2001) in brains from AD patients as well as in cellular and animal models of AD. Biomolecules modified by oxidative stress exist in neurons with or without neurofibrillary tangles and plaques, suggesting that oxidative stress promotes the formation of AD pathologies and is a very early contributor to the disease.

To date, AD pathophysiology remains largely unclear. Recent studies have suggested that epigenetic mechanisms play a key role

* Corresponding author at: 10 Xi Tou Tiao, You An Men Street, Department of Pathology, Capital Medical University, Beijing 100069, P.R. China. Tel.: +86 10 83911698; fax: +86 10 83911699.
E-mail address: newbox111@yahoo.com.cn (L. Li).
[1] These authors contributed equally to this work.

0197-4580/$ – see front matter © 2013 Elsevier Inc. All rights reserved.
http://dx.doi.org/10.1016/j.neurobiolaging.2012.10.013

in the initiation and development of AD (Chouliaras et al., 2010; Zawia et al., 2009). AD is among a few diseases that might display high homocysteine, and low B12 and folate in blood, suggesting that a dysregulation in the S-adenosylmethionine cycle is required for epigenetic regulation through DNA methylation (Fuso et al., 2005). It is worth noting that the expression of *APP* and *BACE1* genes is regulated via methylation of their promoters (Scarpa et al., 2006). Previous studies have demonstrated that AD might begin early in life and involve an interplay among the environment, epigenetics, and oxidative stress. Alterations in the methylation or oxidation of adjacent cytosine-guanine (CpG) dinucleotides within DNA mediate the epigenetic mechanisms that control the gene expression and promote the accumulation of oxidative DNA damage (Zawia et al., 2009). Recent studies of histone acetylation from human postmortem brain samples and transgenic animal models and cell culture demonstrated the conflicting results. Some studies reported that AD is associated with generally increased histone acetylation (Kim et al., 2007; Marambaud et al., 2003), and others showed that a decreased histone acetylation is causally linked to AD. Moreover, some other studies have demonstrated that the memory deficits can be partially recovered by histone deacetylase (HDAC) inhibitor in an AD transgenic mice model (Fischer et al., 2007; Green et al., 2008; Ricobaraza et al., 2009).

The molecular mechanism underlying the promotion of Aβ production by oxidative stress is not completely understood. It has been reported that hydrogen peroxide (H_2O_2) induces APP expression and therefore enhances Aβ production in mammalian lenses (Frederikse et al., 1996). The promoter activity of BACE1 can be potentiated by H_2O_2 at a low concentration, resulting in an enhanced Aβ expression (Tamagno et al., 2005; Tong et al., 2005) in vitro. In this study, we investigated the epigenetic mechanisms (such as DNA methylation and histone acetylation) involved in oxidative stress-induced Aβ overproduction. Because H_2O_2 is the main source of the highly reactive hydroxyl radicals in the brain, human neuroblastoma SH-SY5Y cells, as a more physiological model of neuronal Aβ generation, were treated with H_2O_2 and used as the cell model in our study. We found that H_2O_2 induced the upregulation of *APP* and *BACE1* genes through DNA hypomethylation and histone hperacetylation, correspondingly leading to Aβ overproduction. Our data suggested a novel insight to epigenetic mechanisms, by which oxidative stress might contribute to the AD pathogenesis.

2. Methods

2.1. Cell culture and treatment

Human neuroblastoma SH-SY5Y cells were maintained in Dulbecco's Modified Eagle's Medium (Gibco) supplemented with 10% fetal bovine serum (HyClone), 100 μg/mL streptomycin, and 100 U/mL penicillin (Gibco) at 37 °C in a humidified incubator with 5% CO_2.

Cells were treated with 30% H_2O_2 alone at a dose of 200 μmol/L for 1 hour, or 20 μmol/L for 24 or 72 hours, or in a combination with the following inhibitors. p38-mitogen activated protein kinase (p38MAPK) inhibitor SB203580 (20 μmol/L) and c-Jun amino terminal kinase (JNK) inhibitor SP600125 (10 μmol/L) were used to pretreat the cells for 1 hour before the H_2O_2 treatment. DNA methyltransferase (DNMT) inhibitor 5-Aza-2'-deoxycytidine (5-Aza-dC; 2 μmol/L) was used to treat cells for 72 hours alone or pretreat cells for 72 hours before the H_2O_2 treatment. HDAC inhibitor trichostatin A (TSA; 0.5 μmol/L) was used to treat cells for 24 hours alone or pretreat cells for 24 hours before the H_2O_2 treatment. Cells treated with the same volume of phosphate-buffered saline (PBS) were used as control. The viability of SH-SY5Y cells was evaluated by 3-(4, 5-dimethylthiazol-2-yl)-2, 5-diphenyltetrazolium bromide (MTT) assay.

2.2. Quantification of Aβ level by ELISA

The Aβ level was quantified in cell lysates by enzyme-linked immunosorbent assay (ELISA) using a Biosource kit according to the manufacturer's instructions. Aβ1–40 and Aβ1–42 were evaluated according to the standard curves. The quantity of Aβ in each sample was measured in triplicate. Recombinant C99 was added to the assay to minimize the cross reaction with C99.

2.3. Quantitative real-time PCR

RNA was extracted from cells using SV Total RNA Isolation System (Promega, WI, USA) according to the manufacturer's instructions. Purified RNA was then reversely transcribed into cDNA using Reverse Transcription System (Promega) according to the manufacturer's instructions, and the synthesized cDNA was stored at −20 °C until use. To evaluate the BACE1 expression, quantitative polymerase chain reaction (PCR) was performed on a LightCycler 1.5 instrument (Roche Diagnostics GmbH, Mannheim, Germany). The following primers were used in this study: BACE1, forward primer: GTCGGAGGGAGCATGATCA and reverse primer: CCGCCG GATGGGTGTATAC; and 18S, forward primer: GTAACCCGTTGAA CCCCATT and reverse primer: CCATCCAATCGGTAGTAGCG. Quantitative PCR reactions were conducted in a final volume of 20 μL containing 1 μL of cDNA and SYBR Green PCR Master Mix (Tiangen Biotech Co, LTD, Beijing, China). Briefly, after an initial denaturation step at 95 °C for 7 minutes, the amplification was carried out with 40 cycles at a melting temperature of 95 °C for 45 seconds, an annealing temperature of 62 °C for 35 seconds, and an extension temperature of 72 °C for 60 seconds. Each experiment was performed in triplicate. A dissociation curve was analyzed to assess the amplification specificity. The relative messenger RNA (mRNA) level of the target gene was determined with the $2^{-\triangle\triangle Ct}$ method (LightCycler Software 4.1, Roche Diagnostics GmbH) using 18S as the housekeeping gene.

2.4. Western blot analysis

Cells were harvested and washed with PBS. To obtain the cell lysates, cell pellet was lysed in lysis buffer (50 mmol/L Tris-HCl, 2 mmol/L ethylene diamine tetraacetic acid (EDTA), 2 mmol/L ethylene glycol bis(2-aminoethyl) tetraacetic acid (EGTA), 1 mmol/L dithiothreitol (DTT), 0.1% sodium deoxycholate, 0.5% NP-40, 1 μmol/L sodium orthovanadate, 5 mmol/L sodium pyrophosphate, 5 μg/mL pepstatin A, 5 μg/mL leupeptin, 5 μg/mL aprotinin, 5 μg/mL chymostatin, and 50 nmol/L okadic acid, pH 7.4) and sonicated for 5 minutes. After centrifugation at 13,000 *g* for 10 minutes, the supernatant was collected and stored at −20 °C until use. Protein content was determined using BCA protein assay kit (Pierce). Samples (50 μg per lane for anti-phospho-p38MAPK, anti-phospho-JNK, anti-APP, anti-tumor necrosis factor-alpha convertase [TACE] and anti-methyl-CpG binding domain (MBD) 2; 60 μg per lane for anti-HDAC3 and anti-p300/CBP; 80 μg per lane for anti-DNMT1, anti-DNMT3a, anti-a disintegrin and metalloproteases [ADAM] 10, and anti-BACE1) were loaded in 8%, 10%, or 15% sodium dodecyl sulfate polyacrylamide gel electrophoresis, respectively. After the electrophoresis, proteins were electro-transferred onto nitrocellulose membrane. Blots were blocked with 5% milk in Tris-buffered saline containing 0.1% Tween 20 (TBS-T, pH 7.5) at room temperature for 1 hour and then incubated with primary antibodies in TBS-T at 4 °C overnight. The following primary antibodies were used in this study: rabbit anti-phospho-p38MAPK monoclonal antibody (1:1000, Cell Signaling), rabbit anti-phospho-JNK monoclonal antibody (1:1000, Cell Signaling),

rabbit anti-APP polyclonal antibody (1:1000, Cell Signaling), rabbit anti-HDAC3 monoclonal antibody (1:1000, Cell Signaling), rabbit anti-TACE polyclonal antibody (1:1000, Santa Cruz), mouse anti-ADAM10 monoclonal antibody (1:50; Santa Cruz), rabbit anti-methyl-CpG binding protein 2 (MBD2) polyclonal antibody (1:1000; Santa Cruz), rabbit anti-DNMT1 monoclonal antibody (1:1000; Cell Signaling), rabbit anti-DNMT3a polyclonal antibody (1:1000; Cell Signaling), rabbit anti-BACE1 polyclonal antibody (1:1500; Abcam, London, UK), mouse anti-p300/CBP (p300/ cAMP-response element binding protein) monoclonal antibody (1:250; Abcam, London, UK), and mouse anti-β-actin monoclonal antibody (1:5000, Sigma). Subsequently, blots were washed with TBS-T 3 times and incubated with horseradish peroxidase-conjugated secondary antibody at room temperature for 2 hours. The antibody binding was visualized using Western blot luminol reagent (Santa Cruz) according to the manufacturer's instructions. The signal quantification was carried out using a Gel-Doc Image Scanner (Bio-Rad) and Quantity One software program version 4.2.1 (Bio-Rad). Data in accordance with normal distribution were analyzed by independent *t* test (SPSS 11.5 system, SPSS, Chicago, IL, USA). $p < 0.05$ was considered as statistically significant.

2.5. DNA methylation analysis

Genomic DNA was extracted from cultured cells using Wizard SV Genomic DNA Purification System (Promega) according to manufacturer's instructions. The integrity and purity of DNA were spectrophotometrically examined according to its A260/A280 absorption. A total of 200 ng genomic DNA from each sample was bisulfite-treated with the Methylamp DNA Modification Kit (Epigentek). The quality of bisulfite conversion was evaluated using the PCR products without methyl groups as the control. In order to quantitatively analyze the methylation of APP (GenBank accession number NC_000021) and BACE1 (GenBank accession number NC_000011), the Sequenom MassARRAY platform (CapitalBio, Beijing, China) was used, which consisted of matrix-assisted laser desorption/ionization time-of-flight mass spectrometry and RNA base-specific cleavage (MassCLEAVE). PCR primers were designed by Methprimer (http://epidesigner.com). An additional T7 promoter tag for in vivo transcription was attached to each reverse primer, whereas a 10-mer tag was integrated into the forward primer to correspondingly adjust the melting temperature. Table 1 lists all the primers used in this study. The methylation ratios were generated by Epityper software version 1.0 (Sequenom, San Diego, CA, USA). The generated data were put into the EPI 3.1 Database (EpiData Association, Odense, Denmark) and analyzed with SPSS 11.5 software (McGraw-Hill Inc, New York, NY). Independent *t* tests were conducted to evaluate the difference between the experimental and control groups. $p < 0.05$ was considered statistically significant.

2.6. Nuclear extract and EMSA

Nuclear protein was extracted according to the manufacturer's instructions (Viagene Biotech Co, Ltd). Cultured cells were washed twice with ice-cold PBS (pH 7.6) and once with 1.5 mL cytoplasm lysate I, and then they were lysed with 1.0 mL cytoplasm lysate II. Cell lysates were transferred into to a 1.5-mL vial and centrifuged at 14,000 rpm for 5 minutes at 4 °C. Supernatant was discarded, and the precipitate was washed with 0.5 mL cytoplasm lysate I and centrifuged at 14,000 rpm for 5 minutes at 4 °C. Supernatant was again discarded, and 50 μL nuclear lysate was added to the precipitate. The mixture was incubated at 4 °C for 30 minutes with occasional vibration and then centrifuged at 12,000 rpm for 20 minutes at 4 °C. The precipitate was collected, and the protein content was determined by the BCA protein assay kit.

DNA binding activity of nuclear factor-κB (NF-κB) or specific protein-1/3 (SP1/3) was assayed using nonradioactive electrophoretic gel mobility shift assay (EMSA) kit following the manufacturer's instructions (Viagene Biotech). NF-κB probe (5′-AGTTGAGGG GACTTTCCCAGGC-3′) and SP1/3 probe (5′-ATTCGATCGGGGCG GGGCGAGC-3′) were used in the study. Biotins were labeled in 5′-end of the oligonucleotide. A total of 15 μg crude nuclear protein was incubated in a 15-μL binding reaction system containing 1.5 μL 10× binding buffer, 1.5 μL poly(dI-dC) (1.0 μg/μL) and ddH_2O at room temperature for 20 minutes. Then 0.6 μL Bio-probe (500 fM) was added, and the reaction was incubated at room temperature for 20 minutes. Where indicated, 1 μL and 2 μL of specific competitor (cold oligonucleotide) were added in 50× and 100× competing system before the labeled probe, respectively, and a 20-minute incubation was followed. Nuclear extract from tumor necrosis factor (TNF)-treated (50 ng/mL for 45 minutes) SGC7901 cells (3.6 μg per lane) was used as the NF-κB positive control. Nuclear extract from sodium butyrate-treated (3.0 mmol/L for 6 hours) HCT116 cells (4 μg per lane) was used as the SP1/3 positive control. Protein-DNA complexes were resolved by electrophoresis and subjected to autoradiography. Electrophoresis was carried out on a 6.5% nondenaturing polyacrylamide gel at 175 V in 0.25 × Tris-borate-EDTA (TBE) buffer at 4 °C for 1 hour. Gels were transferred to the banding membrane at 394 mA in 0.5 × TBE buffer at room temperature for 40 minutes. Subsequently, the membrane was cross-linked in an ultraviolet crosslink apparatus for 10 minutes (Immobilization), and steps of blocking, streptavidin-horseradish peroxidase labeling, washing, and membrane equilibration were followed. Finally, images were obtained through the imager apparatus (Alpha Flurechemical).

Table 1
Primer sequences used in this study

Name	Primer sequence
APP-F	aggaagagagGATTCGTTTGGTTTTGAGTTT
APP-R	cagtaatacgactcactatagggagaaggctGCTTCCAAAACAAAAACTAAATC
BACE1-F	aggaagagagTTGGATTATGGTGGTTTGAGTAGTT
BACE1-R	cagtaatacgactcactatagggagaaggctCACAACAAAAACCAAAACAAAACTT

Key: APP, amyloid precursor protein; BACE1, β-site APP-cleaving enzyme 1; F, forward; R, reverse.

2.7. Immunocytochemical staining

Cultured cells were fixed with 4% paraformaldehyde, washed in PBS, and then pretreated with 0.05% Triton-X100 for 5 minutes, 4 M HCl for 15 minutes, and 1% H_2O_2 for 10 minutes. Fixed cells were blocked with 3% bovine serum albumin (BSA) in PBS for 30 minutes and then incubated with mouse monoclonal antibody against 5-methylcytosine (5-mC) (1:300; Epigentek Group Inc) at 4 °C overnight. Cells were washed and then incubated with secondary antibodies of anti-mouse IgG for 2 hours. The immunoreactivity was visualized by the avidin-biotin-peroxidase method (ABC kit, Vector, Burlingame, CA, USA) combined with 0.05% 3,3'-diaminobenzidine and 0.01% H_2O_2 for 5 minutes. Images were obtained with Nikon digital sight DS-Ri1 for Professional Microscopy (Nikon Eclipse 80i). Quantitative immunocytochemical data were obtained from 10 nonoverlapping fields (40×) through 3 independent experiments. Grey values of immunoreactivities were tested using NIS-Elements BR imaging software 3.2.

3. Results

3.1. H_2O_2 induces intracellular accumulation of Aβ in SH-SY5Y cells

Treatments of H_2O_2 (200 μmol/L), SB203580 (20 μmol/L), SP600125 (10 μmol/L), 5-Aza-dC (2 μmol/L), and TSA (0.5 μmol/L) had

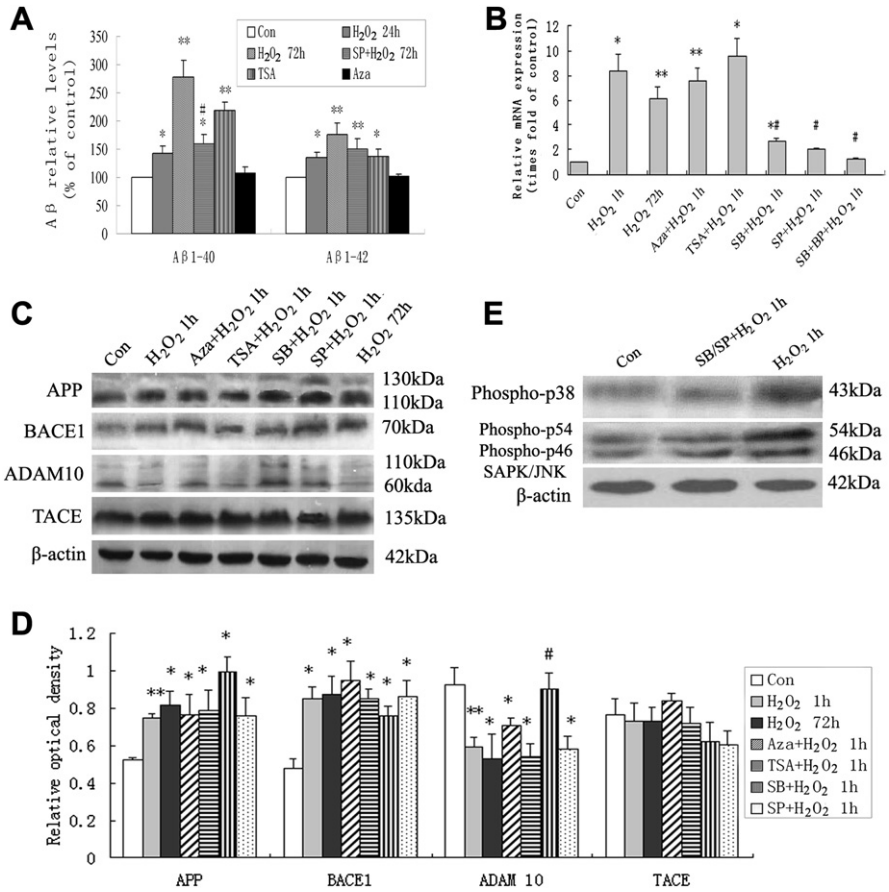

Fig. 1. H_2O_2-induced intracellular generation of amyloid-β (Aβ) in SH-SY5Y cells. (A) Cell lysates of SH-SY5Y cells were assayed using enzyme-linked immunosorbent assay (ELISA). No cross reaction with C99 was observed. Aza, 5-Aza-dC (2 μmol/L) treatment for 72 hours; Con, control; H_2O_2 24 h, H_2O_2 (20 μmol/L) treatment for 24 hours; H_2O_2 72 h, H_2O_2 (20 μmol/L) treatment for 72 hours; SP+ H_2O_2 72 h, SP600125 (10 μmol/L) for 1 hour before H_2O_2 (20 μmol/L) treatment for 72 hours; TSA, trichostatin A (0.5 μmol/L) treatment for 24 hours. Values were expressed as percentage of the Aβ level in the control group. The data were expressed as Mean ± SD. * $p < 0.05$; ** $p < 0.01$ versus control group; # $p < 0.05$ versus H_2O_2 72 hour group ($n = 6$). (B) RNA samples were isolated from the cells for real-time quantitative reverse transcription polymerase chain reaction of β-site amyloid precursor protein (APP)-cleaving enzyme 1 (BACE1) gene. Relative mRNA level quantification of target gene was determined with the $2^{-\triangle\triangle Ct}$ method using the housekeeping gene 18S. The data were shown in mean ± SD (1-way analysis of variance, $n = 6$). The changes of mRNA in experimental groups were normalized by the mean mRNA level in the control group. (C) Homogenates of SH-SY5Y cells were analyzed by Western blot analysis using the antibodies against APP N-terminus (for detecting full-length APP), BACE1, a-disintegrin and metalloproteases (ADAM) 10 and tumor necrosis factor-alpha convertase (TACE). (D) Semiquantitative immunoblot analyses. The blots were then quantified by optical density of the bands after being normalized with the optical density of β-actin bands. The data were expressed as Mean ± SD. * $p < 0.05$; ** $p < 0.01$ versus control group; # $p < 0.05$ versus H_2O_2 1-hour group ($n = 6$). (E) The activation of p38-mitogen activated protein kinase (p38MAPK) and c-Jun amino terminal kinase (JNK) signal pathway was analyzed by Western blot analysis developed with anti-phospho-p38 and phospho-JNK. Con, control; SB/SP+ H_2O_2 1 h, SB203580 (20 μmol/L) treatment 1 hour for p38MAPK test or SP600125 (10 μmol/L) treatment 1 hour for JNK test before H_2O_2 (200 μmol/L) treatment for 1 hour; H_2O_2 1 h, H_2O_2 (200 μmol/L) treatment for 1 hour ($n = 6$).

no effect on the viability of SH-SY5Y cells under the designed conditions. Fig. 1E shows that both p38MAPK and JNK signaling pathways were activated after the H_2O_2 treatment, and the inhibitors had a blockage effect on these 2 pathways. We measured the intracellular levels of Aβ1–40 and Aβ1–42 in SH-SY5Y cells using ELISA. Fig. 1A shows that the Aβ1–40 level was significantly increased (1.77-fold enhancement compared with the control group) after the H_2O_2 treatment for 72 hours, and the JNK signaling pathway inhibitor SP600125 could inhibit this increase. Moreover, 5-Aza-dC had no effect on Aβ production, and TSA could increase Aβ production. Similar trend was observed in Aβ1–42 with slight increment.

Because Aβ accumulation is highly correlated with its precursor protein APP and the APP-cleaving enzymes, we examined the expression of APP and BACE1. Fig. 1B shows that the BACE1 expression at the mRNA level was dramatically increased after the H_2O_2 treatment (1 hour and 72 hours), leading to a 6- to 8-fold enhancement compared with the control group. Both the p38MAPK and JNK signaling pathway inhibitors could separately block this activation. However, a stronger blockage effect was observed when both substances were used in a combination. Pretreatment with 5-Aza-dC slightly blocked the H_2O_2-induced BACE1 upregulation at the mRNA level, whereas it was slightly increased by the pretreatment with TSA.

Fig. 1C and D show that H_2O_2 treatment induced a similar change trend at the protein level although a relatively lower increase was observed. However, the blockage effect of p38MAPK and JNK signaling pathway inhibitors was not significant. To rule out the effects of H_2O_2 on α-secretase, we analyzed the expression of ADAMs. Fig. 1C and D show that the ADAM10 expression was significantly decreased compared with the control group, whereas the pretreatment with 5-Aza-dC or TSA had no significant effect on the H_2O_2-induced ADAM10 expression. Moreover, no obvious change of TACE expression was observed from any treatment. These results indicated that oxidative stress could increase the expression of APP and BACE1 and the activity of β-secretase, resulting in Aβ overproduction.

3.2. H_2O_2 induces hypomethylation of APP and BACE1

To investigate the CpG methylation status of Aβ-related genes under oxidative stress, we examined the methylation levels of

Table 2
Mean methylation levels of APP and BACE1 genes

	Control	H_2O_2 72 h	SP+H_2O_2 72 h
APP methylation level (%)	13.87 ± 0.95	10.52 ± 0.85[a]	12.87 ± 1.10[b]
BACE1 methylation level (%)	3.98 ± 2.34	2.75 ± 0.09[a]	3.78 ± 0.16[b]

Data are expressed as mean ± SD.
Key: APP, amyloid precursor protein; BACE1, β-site APP-cleaving enzyme 1; H_2O_2 72 h, H_2O_2 (20 μmol/L) for 72 hours; SP+H_2O_2 72 h, SP600125 (10 μmol/L) for 1 hour before H_2O_2 (20 μmol/L) treatment for 1 hour.
[a] $p < 0.05$ versus control group.
[b] $p < 0.05$ versus H_2O_2 72 h group ($n = 6$).

APP and BACE1 in the promoter regions by MassARRAY. Using the primers listed in Table 1, APP and BACE1 were amplified from the samples with 72-hour H_2O_2 treatment or without SP600125 pretreatment and the control samples after the bisulfite conversion of genomic DNA. Table 2 shows the mean methylation levels, which were evaluated using Student *t* test. The mean methylation level of BACE1 was lower than that of APP. H_2O_2 could induce the hypomethylation of these 2 specific genes, whereas this modification could be reversed by the JNK signaling pathway inhibitor.

We also evaluated the methylation level of each CpG site within these 2 genes. A total of 65 CpG sites in APP were divided into 31 CpG sites, and 36 CpG sites in BACE1 promoter were divided into 22 CpG sites (Fig. 2). Data of methylation levels revealed a variation at different CpG sites. For *APP* gene (Fig. 2B), the highest methylation level (95%) was located at the first CpG site, whereas the lowest methylation level (nearly 0%) was located at site 63–64. The demethylation was dramatically changed at site 38–40 (decreased to 41.5% of the level in the control samples), and the reverse change of SP600125 was also observed at this site (1.5-fold enhancement compared with the 72-h H_2O_2 treatment group). For *BACE1* gene (Fig. 2D), the highest methylation level (11%) was at the 19–22 CpG site, whereas the lowest methylation level (nearly 0%) was at the 31st CpG site. Similarly, we observed the dramatic demethylation change at the 36th CpG site (decreased to 63.9% of the level from the control samples), and the reverse change of SP600125 was found at the 27th CpG site (1.5-fold enhancement compared with the 72-hour H_2O_2 treatment group). In addition, we did not observe a significant change of methylation level or hypermethylation at some CpG sites in these 2 genes.

3.3. DNA hypomethylation is associated with the decrease of DNMTs

DNA methylation is completed by DNA DNMTs. Because DNA hypomethylation was observed under our experimental conditions, it is highly necessary to investigate whether the change of DNMTs was involved in DNA methylation. In the present study, both DNMT1 and DNMT3a were significantly downregulated after the H_2O_2 treatment for 72 hours, and these downregulations could be reversed by the JNK inhibitor SP600125. However, we did not observe any significant change of MBD2 (Fig. 3G and H). Meanwhile, we also studied the global DNA methylation levels by 5-mC immunocytochemical staining. Table 3 and Fig. 3A–F show that a 1-hour H_2O_2 treatment increased the global DNA methylation level, and the opposite result was obtained by long-term H_2O_2 treatment (72 hours). JNK inhibitor SP600125 could reverse this global DNA hypermethylation, 5-Aza-dC could block the H_2O_2-induced global DNA hypermethylation, and no effect of TSA was observed. These data implied that the oxidative stress could induce the reduction of DNMTs responsible for DNA hypomythelation.

3.4. 5-Aza-dC induces NF-κB DNA binding, and TSA increases NF-κB and SP1/3 DNA binding activities in H_2O_2-treated SH-SY5Y cells

Besides the epigenetic mechanisms involved in the regulation of gene transcription, the stress-activated transcription factors, such as NF-κB and SP1, also play very important roles. To further explore the relationship between the transcription factors and DNA methylation as well as histone acetylation on gene transcription, we tested the DNA binding activities of NF-κB and SP1 in the cells pretreated with 5-Aza-dC or TSA, respectively. Fig. 4 shows that H_2O_2 treatment for 1 hour increased the DNA binding activities of NF-κB and SP1/3 compared with the control in SH-SY5Y cells. Meanwhile, both p38MAPK and JNK signaling pathway inhibitors could reduce their DNA binding activities. Pretreatment with 5-Aza-dC resulted in the increase of NF-κB DNA binding activity, and the SP1/3 DNA binding activity was not affected compared with the single H_2O_2 treatment group. Moreover, TSA pretreatment could increase either NF-κB or SP1/3 DNA binding activity. This result indicated that DNA binding activities of NF-κB and SP1/3 could be regulated by epigenetic changes, and NF-κB might be more sensitive to DNA methylation than SP1/3.

3.5. H_2O_2 might induce global histone hyperacetylation through upregulation of p300/CBP and downregulation of HDAC3

Histone acetylation is correlated with transcriptional activation, and deacetylation is related to transcriptional repression (Richmond and Davey, 2003). Histone acetyltransferases (HATs) catalyze the acetylation of core histones. Coactivators p300 and CBP have been identified as HATs (Ogryzko et al., 1996). Deacetylation catalyzed by HDACs also plays an important role in turning off or maintaining genes in a repressed state. Therefore, we examined the expression level of p300/CBP and HDAC3 by Western blot analysis. Fig. 5 shows that the p300/CBP expression at the protein level was increased in the H_2O_2-treated samples, demonstrating a 2.3-fold enhancement compared with the control samples. However, the HDAC3 expression was decreased to 54.2% of the control samples. JNK inhibitor SP600125 could slightly reverse these 2 reactions. Based on these results, we speculated that the oxidative stress induced the global histone hyperacetylation in an enzyme-dependent manner, which was involved in the process of gene regulation.

4. Discussion

Epigenetics is a major mechanism that accommodates gene expression in response to gene-environment interactions (Morange, 2002). Epigenetics refers to modifications in gene expression affected by DNA methylation and/or chromatin structure, RNA editing and RNA interference without any changes in DNA sequences (Bird, 2002). DNA methylation and histone deacetylation occur shortly after the DNA synthesis, and it can be modified by diverse physiologic or pathologic factors, altering gene expression for the lifetime of the organism. DNA methylation of cytosine is a major epigenetic event affecting the regulation of gene expression, and it has been linked to the process of gene imprinting in mammals. Alterations in 5-methylcytosine patterns on the promoters of genes are the first level of gene regulation in development, differentiation, carcinogenesis, and aging.

Oxidative stress occurs when the oxidative balance is disturbed, that is, excessive production of ROS to cellular antioxidant defenses. The brain is particularly vulnerable to oxidative stress because it is rich in unsaturated fatty acids. The brain consumes much more oxygen compared with other tissues, and it contains less antioxidant enzymes than other organs (Coyle and Puttfarcken, 1993; Floyd and Hensley, 2002). Most AD cases are

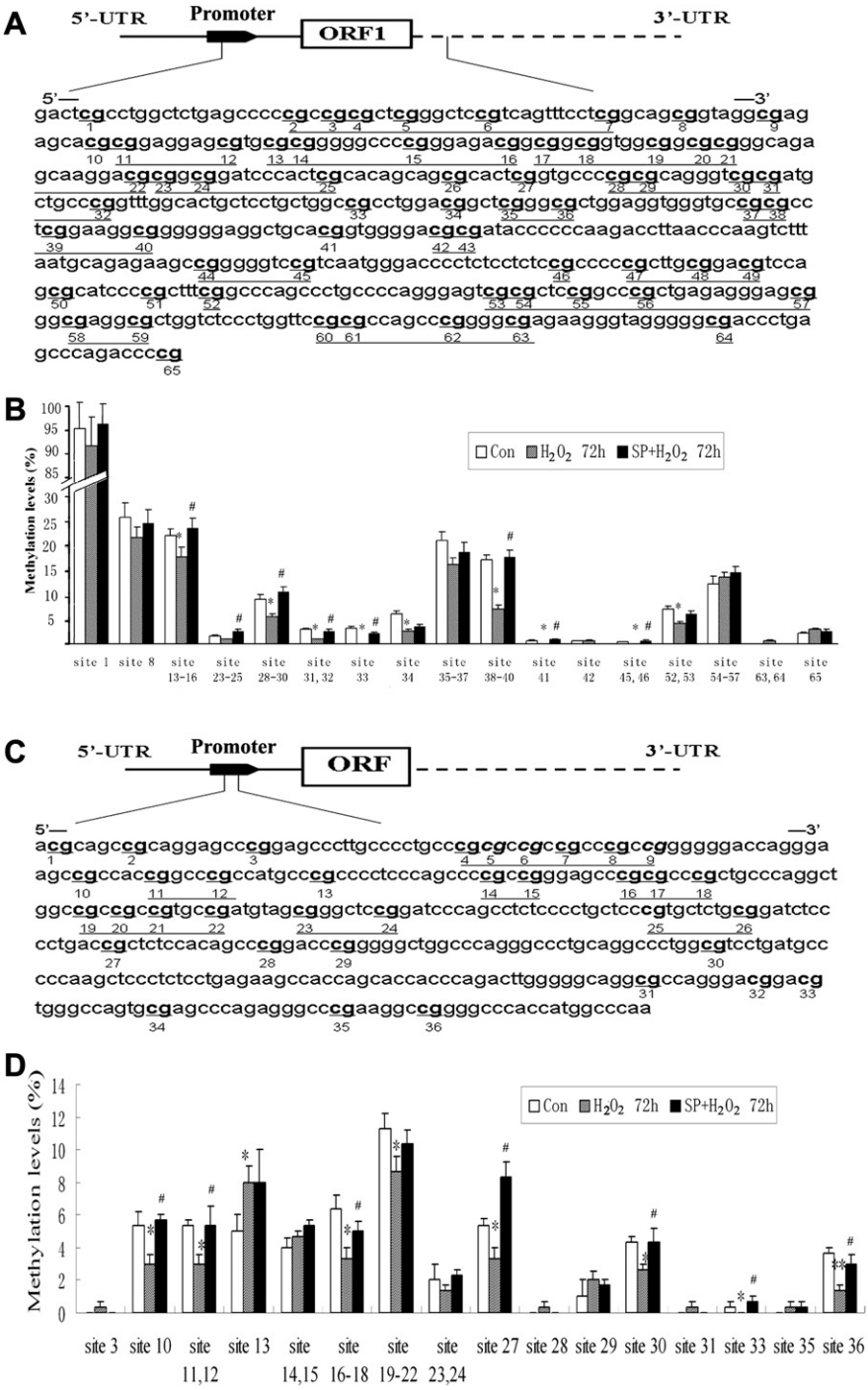

Fig. 2. Methylation levels of *APP* and *BACE1* genes. Schematic diagram of amyloid precursor protein (APP) (A) and β-site APP-cleaving enzyme 1 (BACE1) (C). The transcripts were composed of a 5′-untranslated region (UTR) with internal promoter activity, open reading frame (ORF), and a 3′-UTR. (A) The sequence represents a 539-base pair (bp) fragment (bps between −192 and 346) in *APP* gene. (C) The sequence represents a 397-bp fragment (bps between −388 and 2) in *BACE1* gene. Polymerase chain reaction primers were designed on the basis of the reverse complementary strands of these fragments. Numbers refer to the locations of cytosine-guanine (CpG) sites and underlining highlights of CpG sites include more than 1 CpG site tested at the same time. (B, D) Mean methylation levels of CpG sites in APP and BACE1. Methylation levels of all CpG sites in each gene were compared between samples from the control (Con) group without treatment and experimental groups treated with H_2O_2 (20 μmol/L) for 72 hours (H_2O_2 72 h) and SP600125 (10 μmol/L) for 1 hour before H_2O_2 (20 μmol/L) treatment for 72 hours (SP+H_2O_2 72 h). The Sequenom MassARRAY platform was used for quantitative methylation analysis. (B) CpG sites were numbered as 1–65 from the 5′ end to 3′ end in *APP* gene. (D) CpG sites were numbered as 3–36 from the 5′ end to the 3′ end in *BACE1* gene. The CpG sites which were not shown did not exhibit obvious methylation signals. The data were expressed as mean ± SD. * $p < 0.05$; ** $p < 0.01$ versus control group; # $p < 0.05$ versus H_2O_2 72 h group ($n = 6$).

sporadic with late onset (later than 65 years old), and their causes remain unclear. The major risk factors for sporadic AD include aging, atherosclerosis, diabetes mellitus, stroke, Apolipoprotein E ε4, and less education. Accumulating evidence suggests that oxidative stress is an early event in AD. ROS results from several cellular insults including aging, hyperglycemia, and hypoxic insults, which are all well known risk factors for AD development (Guglielmotto et al., 2010). It seems that mitochondria are the

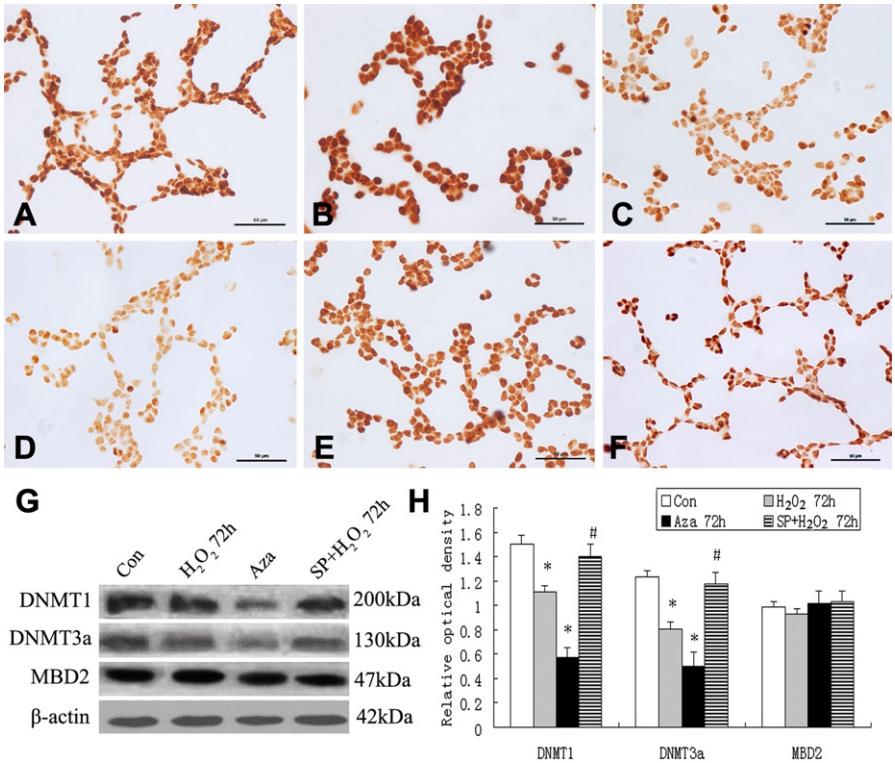

Fig. 3. Global DNA methylation levels and changes of DNA methylation related enzymes. Global DNA methylation levels were evaluated by immunocytochemical staining. 5-methylcytosine (5-mC) immunoreactivity was located in the cell nucleus. (A) control, (B) H_2O_2 treatment (200 μmol/L) for 1 hour, (C) H_2O_2 (20 μmol/L) for 72 hours, (D) 5-Aza-2'-deoxycytidine (5-Aza-dC) (2 μmol/L) for 72 hours before H_2O_2 (200 μmol/L) treatment for 1 hour, (E) trichostatin A (TSA) (0.5 μmol/L) for 24 hours before H_2O_2 (200 μmol/L) treatment for 1 hour, (F) SP600125 (10 μmol/L) for 1 hour before H_2O_2 (200 μmol/L) treatment for 1 hour. Scale bar = 50 μm. (G, H) Western blot analysis of DNA methyltransferase (DNMT)1, DNMT3a, and MBD2. Homogenates of SH-SY5Y cells from the control (Con) group without treatment and experimental groups treated with H_2O_2 (20 μmol/L) for 72 hours (H_2O_2 72 h), 5-Aza-dC (2 μmol/L) for 72 hours (Aza), and SP600125 (10 μmol/L) for 1 hour before H_2O_2 (20 μmol/L) treatment for 72 hours (SP+ H_2O_2 72 h) were analyzed by Western blot analysis using antibodies against DNMT1, DNMT3a, or MBD2. The blots were densitometrically quantified, and the data after being normalized with the β-actin blots were shown in mean ± SD ($n = 6$). * $p < 0.05$ versus control group, # $p < 0.05$ versus H_2O_2 72 h group.

major source of radicals under pathologic conditions. For example, monoamine oxidase is located in the outer membrane of mitochondria, and it participates in the degradation of neurotransmitters, leading to H_2O_2 generation (Werner and Cohen, 1991). In CpG dinucleotides, cytosine is the preferred base for DNA methylation, whereas guanine is the site for oxidative damage. Few studies have addressed the DNA methylation and DNA oxidative damage simultaneously as an epigenetic phenomenon. However, little is known on how DNA methylation and DNA oxidation interact with each other. Previous studies found that oxidation of guanine in CpG dinucleotide reduces the MBD binding (Valinluck et al., 2004). When 5-methylcytosine is oxidized to 5-hydroxymethylcytosine (5-hmC), its affinity to MBD is greatly reduced to the same level as unmethylated cytosine. Therefore, methylated CpG has been found to account for decreased transcription factor binding to the promoter region (Clark et al., 1997; Zhu et al., 2003). Recently, various studies have shown that high levels of 5-hmC are present in the brain (Munzel et al., 2010). Compared with 5-mC, 5-hmC has a lower affinity to methyl binding proteins, suggesting that it plays a different role in the regulation of gene expression, and it is also involved in the DNA demethylation process (Ficz et al., 2011; Munzel et al., 2011). As a newly described epigenetic modification, the increase of 5-mC and 5-hmC in mouse hippocampus is age-related, suggesting that 5-hmC plays an important role in the etiology and course of age-related neurodegenerative disorders (Chouliaras et al., 2012a, 2012b; van den Hove et al., 2012).

In the present study, we found that the level of DNA methylation in promoters of *APP* and *BACE1* genes was decreased after the H_2O_2 treatment, the JNK signaling pathway inhibitor could reverse this change, and the same change for global DNA methylation was also observed. Because H_2O_2 synchronously promotes the phosphor-activation of several distinct protein kinase cascades, including p38MAPK and JNK, this result suggested that the oxidative stress

Table 3
Mean gray values of 5-mC immunoreactivity staining

Control	H_2O_2 1 h	H_2O_2 72 h	Aza+H_2O_2 1 h	TSA+H_2O_2 1 h	SP+H_2O_2 1 h
103.67 ± 19.34	75.88 ± 9.79[a]	131.98 ± 10.28[a]	146.56 ± 11.16[a,b]	105.43 ± 13.08[b]	115.06 ± 13.46[b]

Data are expressed as mean ± SD. Lower gray values correspond with greater staining.
Key: 5-mC, 5-methylcytosine; Aza+H_2O_2 1 h, 5-Aza-dC (2 μmol/L) for 72 hours before H_2O_2 (200 μmol/L) treatment for 1 hour; H_2O_2 1 h, H_2O_2 (200 μmol/L) treatment for 1 hour; H_2O_2 72 h, H_2O_2 (20 μmol/L) for 72 hours; SP+H_2O_2 1 h, SP600125 (10 μmol/L) for 1 hour before H_2O_2 (200 μmol/L) treatment for 1 hour; TSA+H_2O_2 1 h, trichostatin A (0.5 μmol/L) for 24 hours before H_2O_2 (200 μmol/L) treatment for 1 hour;
[a] $p < 0.01$ versus control group.
[b] $p < 0.05$ versus H_2O_2 1-h group ($n = 6$).

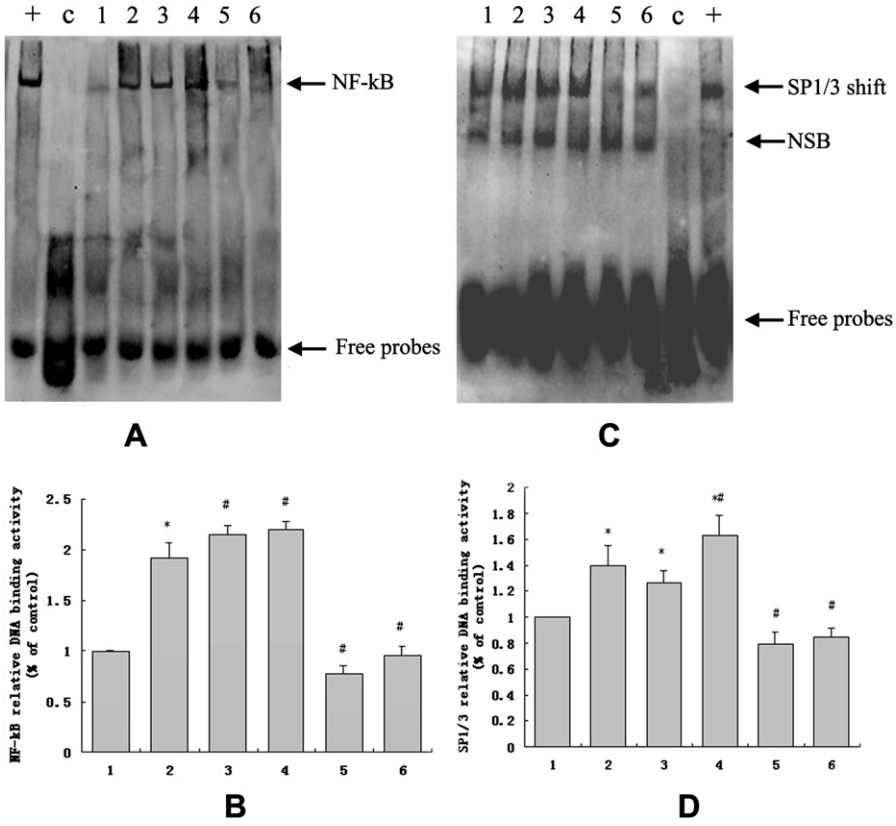

Fig. 4. (EMSA) of nuclear extracts isolated from SH-SY5Y cells showing nuclear binding of nuclear factor-κB (NF-κB) or specific protein-1/3 (SP1/3) after various treatments. Nuclear extracts were prepared and analyzed by EMSA using nonradioactive-labeled NF-κB or SP1/3 oligonucleotide. The formed DNA-protein complexes are indicative of NF-κB (A) or SP1/3 (C) specific band (arrow) after exposure of SH-SY5Y cells to 1, phosphate-buffered saline (PBS) (control); 2, H_2O_2 (200 μmol/L) treatment for 1 hour; 3, 5-Aza-2'-deoxycytidine (5-Aza-dC) (2 μmol/L) for 72 hours before H_2O_2 (200 μmol/L) treatment for 1 hour; 4, trichostatin A (TSA) (0.5 μmol/L) for 24 hours before H_2O_2 (200 μmol/L) treatment for 1 hour; 5, SB203580 (20 μmol/L) for 1 hour before H_2O_2 (200 μmol/L) treatment for 1 hour; 6, SP600125 (10 μmol/L) for 1 hour before H_2O_2 (200 μmol/L) treatment for 1 hour; +, positive control; c, cold oligonucleotide. Densitometric quantitation of specific NF-κB (B) or SP1/3 (D) binding was compared with the control values set at 100%. The histograms represent the mean values and the error bars SD of the relative intensity of the bands of 3 experiments. * $p < 0.05$ versus control group (1); # $p < 0.05$ versus H_2O_2 1-hour group (2).

could induce DNA hypomethylation of global genes as well as specific AD-related genes. It is reported that *APP* (Mani and Thakur, 2006; West et al., 1995), *BACE* and *PS1* (Fuso et al., 2005) genes all contain manipulable, methylated CpG sites. A case study has reported the complete demethylation of the *APP* gene in an AD postmortem cortical sample, but not in similar samples from a normal control subject (West et al., 1995). The cytosine-guanine (CG) content of the APP promoter is approximately 72%, and the rate of CpG dinucleotides is increased by 5 times compared with other eukaryotic promoters, indicating that its expression is regulated by DNA methylation (Hoffman and Chernak 1995; Querfurth et al., 1999). Few studies have examined the methylcytosine levels on the APP promoter, and previous studies have provided various results depending on the region of the promoter (Nagane et al., 2000; Rogaev et al., 1994; Tohgi et al., 1999). In this study, we showed that 65 CpG sites were located in APP promoter region and the first exon, and the BACE1 promoter region consisted of 36 CpG sites. Methylation levels revealed a variation at different CpG sites.

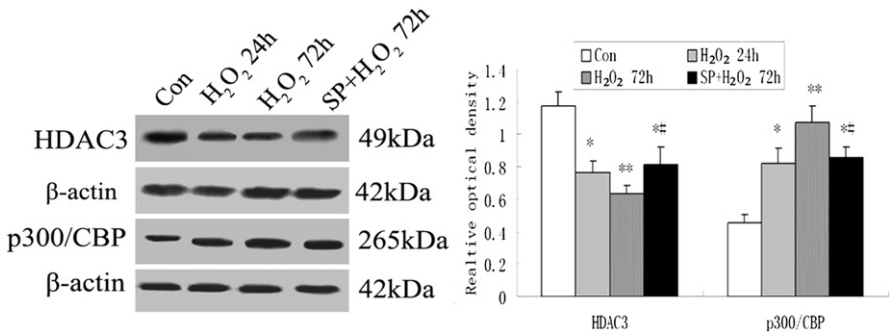

Fig. 5. Western blot analysis of p300/CBP and histone deacetylase (HDAC)3. Homogenates of SH-SY5Y cells from the control (Con) group without treatment and experimental groups treated with H_2O_2 (20 μmol/L) for 24 hours (H_2O_2 24 h), H_2O_2 (20 μmol/L) for 72 hours (H_2O_2 72 h), and SP600125 (10 μmol/L) for 1 hour before H_2O_2 (20 μmol/L) treatment for 72 hours (SP+ H_2O_2 72 h) were analyzed by Western blot analysis using antibodies against p300/CBP or HDAC3. The blots were densitometrically quantified, and the data after being normalized with the β-actin blots were shown in mean ± SD ($n = 6$). * $p < 0.05$, ** $p < 0.01$ versus control group, # $p < 0.05$ versus H_2O_2 72 h group.

Bisulfite conversion of DNA is widely used to the detect DNA methylation. However, it has recently been shown that this approach is not able to discriminate 5-mC from 5-hmC (Jin et al., 2010; Nestor et al., 2010). Therefore, all results using such methods should be treated with caution, as the presence of 5-hmC might be underestimated or mistaken as 5-mC. Currently, numerous novel techniques have been developed for specific and reliable detection and quantification of 5-hmC. However, none of these approaches has been fully optimized, and all the currently available techniques have advantages and disadvantages (van den Hove et al., 2012). In this experiment, we used the bisulfite conversion of DNA to detect methylation levels. It is reported that 5-hmC is particularly enriched in gene promoters and intragenic regions. Moreover, 5-hmC in the promoter region is correlated with gene expression only in promoters with low, but not intermediate or high CpG content (Jin et al., 2011a), and the 5-hmC content is varied according to the cellular types (Haffner et al., 2011; Nestor et al., 2012). The terminally differentiated cells (lack of cell division), such as neurons, have a high level of 5-hmC, the proliferative cells (less differentiated cell), such as stem/progenitor cells or tumor cells, have a very low level of 5-hmC. Jin et al. (2011b) reported that 5-hmC is remarkably depleted in many cancer types. In brain tumors, 5-hmC demonstrates an even more drastic reduction, which is up to more than 30-fold lower than that in the normal brain. Based on these findings, because the SH-SY5Y cell is a type of nerve tissue-originated tumor cell and the promoter sections examined in this experiment are enriched with CpG, 5-hmC content should be low enough to be ignored. Therefore, our present results are acceptable.

DNA methylation completed by DNMTs has 2 methylation patterns. The methylation maintenance is essential to preserve DNA methylation patterns in the cellular DNA replication cycle, and it is catalyzed by DNMT1. DNMT3a and DNMT3b are the de novo DNMTs to establish DNA methylation patterns during early development (Abel and Zukin, 2008; Mehler, 2008). Our experimental results revealed that the expression of both types of DNMTs was decreased under the H_2O_2 treatment, and the JNK signaling pathway inhibitor could reverse these downregulations, suggesting that the DNMTs were involved in DNA hypomethylation under the oxidative stress condition. It is assumed that DNA methylation might act as a negative transcription regulator. There are 3 possible mechanisms proposed for transcriptional repression by DNA methylation (Singal and Ginder, 1999). The first mechanism involves direct interference with the binding of specific transcription factors to their recognition sites in their respective promoters. Several transcription factors, including activator protein-2 (AP-2), c-Myc/Myn, adenovirus E2 factor (E2F) and NF-κB, recognize the sequences containing CpG residues, and their binding is inhibited by methylation. In contrast, other transcription factors (such as SP1 and CCAAT-box-binding transcription factors (CTF)) are not sensitive to methylation of their binding sites (Tate and Bird, 1993), and many factors have no CpG dinucleotide residues in their binding sites. NF-κB, a redox-sensitive transcription factor, plays an important role in proinflammatory and protective pathways, including transcription of cytokine genes and antioxidant genes (Baeuerle and Baltimore, 1996; Memet, 2006). SP1 is also a redox-sensitive transcription factor, and its DNA binding activity is modulated by the cellular redox state. SP1 is also likely to regulate genes that are involved in glucose metabolism, such as the tricarboxylic acid (TCA) circle (Ammendola et al., 1994). It is confirmed that APP and BACE1 promoters contain a number of putative transcription factor binding sites, including SP1, NF-κB, Yin Yang 1 (YY1), myeloid zinc finger 1 (MZF1) and hepatocyte nuclear factor 3b (HNF-3b) (Christensen et al., 2004; Grilli et al., 1995; Hoffman and Chernak, 1995). Our EMSA result revealed that H_2O_2 treatment could increase the DNA binding activities of NF-κB and SP1, and this binding activity could be blocked by either the p38MAPK or JNK signaling pathway inhibitor. Moreover, DNA demethylation could increase the NF-κB DNA binding activity, and it had no effect on that of SP1. The result was consistent with the previous study that NF-κB might be more sensitive to DNA methylation change than SP1. The other potential mechanism for methylation-induced silencing is through the direct binding of specific transcriptional repressors to methylated DNA. Two such factors, methyl cytosine binding protein 1 and 2, have been identified, and their binding to methylated CpG residues has been shown in any sequence context. The MBD family seems to be linked to the DNA methylation pattern (Jaenisch and Bird, 2003). MBD proteins act as transcriptional repressors and promote the gene-silencing effect of DNA methylation by recruiting multiprotein repressor complexes containing HDACs and nucleosome-remodeling activities into inhibitory chromatin structures. MBD2 is a 40 kDa protein with demethylase activity, and it transforms methylated cytosine bases to cytosine (Bhattacharya et al., 1999). In the present study, we found that the MBD2 expression was not affected by oxidative stress. In addition, more attention should be paid to ten-eleven translocation (TET) family of enzymes that catalyze 5-mC to 5-hmC. The TET1 enzyme acts as transcriptional repressor by binding to CpG islands and then catalyzing the conversion of 5-mC to 5-hmC (Williams et al., 2011), or by binding to polycomb target genes and the sin3a repressor complex (Wu et al., 2011). It remains unknown the exact stimuli that induce the TET-mediated conversion of 5-mC to 5-hmC.

Condensation of eukaryotic DNA in chromatin suppresses gene activity through the coiling of DNA on the surface of the nucleosome core and the folding of nucleosome assemblies, thus decreasing the accessibility to the transcriptional apparatus (Wu, 1997). Tightly bound DNA around a nucleosome core (histone residues H2A, H2B, H3, and H4) suppresses the gene transcription by decreasing the accessibility of transcription factors (such as NF-κB and AP-1) to the transcriptional complex. Acetylation of lysine residues in the N-terminal tails of the core histone proteins results in the DNA uncoiling, allowing increased accessibility for transcription factor binding (Wu, 1997). Acetylation of lysine (K) residues on histone 4 (K5, K8, K12, and K16) is thought to be directly related to the regulation of gene transcription (Bannister and Miska, 2000; Imhof and Wolffe, 1998). Histone acetylation is reversible, and it is regulated by a group of HATs that promote acetylation and HDACs that promote deacetylation. It has been reported that CBP/p300, which is regulated by mitogen activated protein kinase pathways, is vital for the coactivation of several transcription factors (including NF-κB and AP-1) in the transcription machinery (Ogryzko et al., 1996; Thomson et al., 1999). These activation complexes initiate the transcription with RNA polymerase II (Kamei et al., 1996; Ng et al., 1997). Our present data revealed that H_2O_2 induced the upregulation of p300/CBP and downregulation of HDAC3, which might induce enzyme-dependent global histone hyperacetylation. Meanwhile, we found that pretreatment with HDAC inhibitor TSA could increase either NF-κB or SP1/3 DNA binding activity. Therefore, histone hyperacetylation via CBP/p300 and/or HDAC might play a significant role in the activation of NF-κB/SP1-mediated gene expression for Aβ production under the oxidative stress.

Our quantitative PCR results were basically consistent with these epigenetic changes. Moreover, the result of specific gene methylation level revealed a variation at different CpG sites, and the significant changes were limited to 53%–56% CpG dinucleotide residues. It is difficult to estimate the relative contributions of DNA hypomethylation, histone acetylation, and transcription factors in gene transcription. Moreover, further studies are necessary to identify key sites. However, we were not satisfied with the Western blot analysis results, which indicated that the mRNA translation was

more complicated, and it was regulated by more factors. Of course, these results on H_2O_2 were not only specific for *APP* and *BACE1* genes, but we only investigated these genes in this study because of their relation with Aβ production. Meanwhile, we found that the β-secretase pathway took preference to result in an increase of Aβ production, and the intracellular Aβ1–40 accumulation was much more than that of Aβ1–42. The generation of Aβ1–40 or Aβ1–42 depends on the cleavage site of γ-secretase. Usually, mutant *PS1* leads to the overproduction of Aβ1–42 in familial AD patients. Our present results showed that intracellular Aβ1–40 was accumulated, suggesting that *PS1* functioned as a normal way under the current culture condition. However, we did not detect the secreted Aβ1–40 or Aβ1–42 in the culture media either by ELISA or by immunoprecipitation (data not shown). This result suggested that our SH-SY5Y cells lost the capability of secreting detectable amounts of Aβ into the culture medium. Misonou et al. (2000) have reported the similar result, and they demonstrated that H_2O_2-oxidative stress causes an increased level of intracellular Aβ in SH-SY5Y cells through enhancing the amyloidogenic pathway.

In the present study, we reported that oxidative stress resulted in an imbalance between DNA methylation and demethylation as well as histone acetylation and deacetylation associated with transcription factors activation, leading to the transcription of AD-related genes with Aβ overproduction. Our study suggests a potential mechanism for oxidative stress response, which might contribute to the pathogenesis and development of AD.

Disclosure statement

The authors declare that they have no conflicts of interest.

Acknowledgements

This work was supported by Beijing Natural Science Foundation (No. 7102012), National Natural Science Foundation (No. 8107092), the Beijing Education Committee of Science and Technology Plan Projects (No. KM201110025006), and China 973 Preprogram (2011CB512109).

References

Abel, T., Zukin, R.S., 2008. Epigenetic targets of HDAC inhibition in neurodegenerative and psychiatric disorders. Curr. Opin. Pharmacol. 8, 57–64.
Ammendola, R., Mesuraca, M., Russo, T., Cimino, F., 1994. The DNA-binding efficiency of Sp1 is affected by redox changes. Eur. J. Biochem. 225, 483–489.
Baeuerle, P.A., Baltimore, D., 1996. NF-kappa B: ten years after. Cell 87, 13–20.
Bannister, A.J., Miska, E.A., 2000. Regulation of gene expression by transcription factor acetylation. Cell. Mol. Life Sci. 57, 1184–1192.
Barja, G., 2004. Free radicals and aging. Trends. Neurosci. 27, 595–600.
Bhattacharya, S.K., Ramchandani, S., Cervoni, N., Szyf, M., 1999. A mammalian protein with specific demethylase activity for mCpG DNA. Nature 397, 579–583.
Bird, A., 2002. DNA methylation patterns and epigenetic memory. Genes Dev. 16, 6–21.
Chouliaras, L., Rutten, B.P., Kenis, G., Peerbooms, O., Visser, P.J., Verhey, F., van Os, J., Steinbusch, H.W., van den Hove, D.L., 2010. Epigenetic regulation in the pathophysiology of Alzheimer's disease. Prog. Neurobiol. 90, 498–510.
Chouliaras, L., van den Hove, D.L., Kenis, G., Keitel, S., Hof, P.R., van Os, J., Steinbusch, H.W., Schmitz, C., Rutten, B.P., 2012a. Age-related increase in levels of 5-hydroxymethylcytosine in mouse hippocampus is prevented by caloric restriction. Curr. Alzheimer Res. 9, 536–544.
Chouliaras, L., van den Hove, D.L., Kenis, G., Keitel, S., Hof, P.R., van Os, J., Steinbusch, H.W., Schmitz, C., Rutten, B.P., 2012b. Prevention of age-related changes in hippocampal levels of 5-methylcytidine by caloric restriction. Neurobiol. Aging 33, 1672–1681.
Christensen, M.A., Zhou, W., Qing, H., Lehman, A., Philipsen, S., Song, W., 2004. Transcriptional regulation of BACE1, the beta-amyloid precursor protein beta-secretase, by Sp1. Mol. Cell Biol. 24, 865–874.
Clark, S.J., Harrison, J., Molloy, P.L., 1997. Sp1 binding is inhibited by (m)Cp(m)CpG methylation. Gene 195, 67–71.
Coyle, J.T., Puttfarcken, P., 1993. Oxidative stress, glutamate, and neurodegenerative disorders. Science 262, 689–695.
Ficz, G., Branco, M.R., Seisenberger, S., Santos, F., Krueger, F., Hore, T.A., Marques, C.J., Andrews, S., Reik, W., 2011. Dynamic regulation of 5-hydroxymethylcytosine in mouse ES cells and during differentiation. Nature 19, 398–402.
Fischer, A., Sananbenesi, F., Wang, X., Dobbin, M., Tsai, L.H., 2007. Recovery of learning and memory is associated with chromatin remodelling. Nature 447, 178–182.
Floyd, R.A., Hensley, K., 2002. Oxidative stress in brain aging. Implications for therapeutics of neurodegenerative diseases. Neurobiol. Aging 23, 795–807.
Frederikse, P.H., Garland, D., Zigler Jr., J.S., Piatigorsky, J., 1996. Oxidative stress increases production of beta-amyloid precursor protein and beta-amyloid (Abeta) in mammalian lenses, and Abeta has toxic effects on lens epithelial cells. J. Biol. Chem. 271, 10169–10174.
Fuso, A., Seminara, L., Cavallaro, R.A., D'Anselmi, F., Scarpa, S., 2005. S-adenosylmethionine/ homocysteine cycle alterations modify DNA methylation status with consequent deregulation of PS1 and BACE and beta-amyloid production. Mol. Cell. Neurosci. 28, 195–204.
Green, K.N., Steffan, J.S., Martinez-Coria, H., Sun, X., Schreiber, S.S., Thompson, L.M., LaFerla, F.M., 2008. Nicotinamide restores cognition in Alzheimer's disease transgenic mice via a mechanism involving sirtuin inhibition and selective reduction of Thr231-phosphotau. J. Neurosci. 28, 11500–11510.
Grilli, M., Ribola, M., Alberici, A., Valerio, A., Memo, M., Spano, P., 1995. Identification and characterization of a kappa B/Rel binding site in the regulatory region of the amyloid precursor protein gene. J. Biol. Chem. 270, 26774–26777.
Guglielmotto, M., Giliberto, L., Tamagno, E., Tabaton, M., 2010. Oxidative stress mediates the pathogenic effect of different Alzheimer's disease risk factors. Front. Aging Neurosci. 2, 1–8.
Haffner, M.C., Chaux, A., Meeker, A.K., Esopi, D.M., Gerber, J., Pellakuru, L.G., Toubaji, A., Argani, P., Iacobuzio-Donahue, C., Nelson, W.G., Netto, G.J., De Marzo, A.M., Yegnasubramanian, S., 2011. Global 5-hydroxymethylcytosine content is significantly reduced in tissue stem/progenitor cell compartments and in human cancers. Oncotarget 2, 627–637.
Hoffman, P.W., Chernak, J.M., 1995. DNA binding and regulatory effects of transcription factors SP1 and USF at the rat amyloid precursor protein gene promoter. Nucleic Acids Res. 23, 2229–2235.
Imhof, A., Wolffe, A.P., 1998. Transcription: gene control by targeted histone acetylation. Curr. Biol. 8, R422–R424.
Jaenisch, R., Bird, A., 2003. Epigenetic regulation of gene expression: how the genome integrates intrinsic and environmental signals. Nat. Genet. 33 (suppl), 245–254.
Jin, S.G., Jiang, Y., Qiu, R., Rauch, T.A., Wang, Y., Schackert, G., Krex, D., Lu, Q., Pfeifer, G.P., 2011a. 5-Hydroxymethylcytosine is strongly depleted in human cancers but its levels do not correlate with IDH1 mutations. Cancer Res. 15, 7360–7365.
Jin, S.G., Kadam, S., Pfeifer, G.P., 2010. Examination of the specificity of DNA methylation profiling techniques towards 5-methylcytosine and 5-hydroxymethylcytosine. Nucleic Acids Res. 38, e125.
Jin, S.G., Wu, X., Li, A.X., Pfeifer, G.P., 2011b. Genomic mapping of 5-hydroxymethylcytosine in the human brain. Nucleic Acids Res. 39, 5015–5024.
Kamei, Y., Xu, L., Heinzel, T., Torchia, J., Kurokawa, R., Gloss, B., Lin, S.C., Heyman, R.A., Rose, D.W., Glass, C.K., Rosenfeld, M.G., 1996. A CBP integrator complex mediates transcriptional activation and AP-1 inhibition by nuclear receptors. Cell 85, 403–414.
Kim, D., Nguyen, M.D., Dobbin, M.M., Fischer, A., Sananbenesi, F., Rodgers, J.T., Delalle, I., Baur, J.A., Sui, G., Armour, S.M., Puigserver, P., Sinclair, D.A., Tsai, L.H., 2007. SIRT1 deacetylase protects against neurodegeneration in models for Alzheimer's disease and amyotrophic lateral sclerosis. EMBO J. 26, 3169–3179.
Mani, S.T., Thakur, M.K., 2006. In the cerebral cortex of female and male mice, amyloid precursor protein (APP) promoter methylation is higher in females and differentially regulated by sex steroids. Brain Res. 1067, 43–47.
Marambaud, P., Wen, P.H., Dutt, A., Shioi, J., Takashima, A., Siman, R., Robakis, N.K., 2003. A CBP binding transcriptional repressor produced by the PS1/epsilon-cleavage of N-cadherin is inhibited by PS1 FAD mutations. Cell 114, 635–645.
Mehler, M.F., 2008. Epigenetic principles and mechanisms underlying nervous system functions in health and disease. Prog. Neurobiol. 86, 305–341.
Memet, S., 2006. NF-kappaB functions in the nervous system: from development to disease. Biochem. Pharmacol. 72, 1180–1195.
Misonou, H., Morishima-Kawashima, M., Ihara, Y., 2000. Oxidative stress induces intracellular accumulation of amyloid beta-protein (Abeta) in human neuroblastoma cells. Biochemistry 39, 6951–6959.
Montine, T.J., Amarnath, V., Martin, M.E., Strittmatter, W.J., Graham, D.G., 1996. E-4-hydroxy-2-nonenal is cytotoxic and cross-links cytoskeletal proteins in P19 neuroglial cultures. Am. J. Pathol. 148, 89–93.
Morange, M., 2002. The relations between genetics and epigenetics: a historical point of view. Ann. N. Y. Acad. Sci. 981, 50–60.
Munzel, M., Globisch, D., Bruckl, T., Wagner, M., Welzmiller, V., Michalakis, S., Müller, M., Biel, M., Carell, T., 2010. Quantification of the sixth DNA base hydroxymethylcytosine in the brain. Angew. Chem. Int. Ed. Engl. 4931, 5375–5377.
Munzel, M., Globisch, D., Carell, T., 2011. 5-Hydroxymethylcytosine, the sixth base of the genome. Angew. Chem. Int. Ed. Engl. 11, 6460–6468.
Nagane, Y., Utsugisawa, K., Tohgi, H., 2000. PCR amplification in bisulfite methylcytosine mapping in the GC-rich promoter region of amyloid precursor protein gene in autopsy human brain. Brain Res. Brain Res. Protoc. 5, 167–171.
Nestor, C.E., Ottaviano, R., Reddington, J., Sproul, D., Reinhardt, D., Dunican, D., Katz, E., Dixon, J.M., Harrison, D.J., Meehan, R.R., 2012. Tissue type is a major

modifier of the 5-hydroxymethylcytosine content of human genes. Genome Res. 22, 467–477.
Nestor, C., Ruzov, A., Meehan, R., Dunican, D., 2010. Enzymatic approaches and bisulfite sequencing cannot distinguish between 5-methylcytosine and 5-hydroxymethylcytosine in DNA. Biotechniques 484, 317–319.
Ng, K.W., Ridgway, P., Cohen, D.R., Tremethick, D.J., 1997. The binding of a Fos/Jun heterodimer can completely disrupt the structure of a nucleosome. EMBO J. 16, 2072–2085.
Nunomura, A., Chiba, S., Lippa, C.F., Cras, P., Kalaria, R.N., Takeda, A., Honda, K., Smith, M.A., Perry, G., 2004. Neuronal RNA oxidation is a prominent feature of familial Alzheimer's disease. Neurobiol. Dis. 17, 108–113.
Nunomura, A., Perry, G., Aliev, G., Hirai, K., Takeda, A., Balraj, E.K., Jones, P.K., Ghanbari, H., Wataya, T., Shimohama, S., Chiba, S., Atwood, C.S., Petersen, R.B., Smith, M.A., 2001. Oxidative damage is the earliest event in Alzheimer disease. J. Neuropathol. Exp. Neurol. 60, 759–767.
Ogryzko, V.V., Schiltz, R.L., Russanova, V., Howard, B.H., Nakatani, Y., 1996. The transcriptional coactivators p300 and CBP are histone acetyltransferases. Cell 87, 953–959.
Querfurth, H.W., Jiang, J., Xia, W., Selkoe, D.J., 1999. Enhancer function and novel DNA binding protein activity in the near upstream beta APP gene promoter. Gene 232, 125–141.
Richmond, T.J., Davey, C.A., 2003. The structure of DNA in the nucleosome core. Nature 423, 145–150.
Ricobaraza, A., Cuadrado-Tejedor, M., Perez-Mediavilla, A., Frechilla, D., Del Rio, J., Garcia-Osta, A., 2009. Phenylbutyrate ameliorates cognitive deficit and reduces tau pathology in an Alzheimer's disease mouse model. Neuropsychopharmacology 34, 1721–1732.
Rogaev, E.I., Lukiw, W.J., Lavrushina, O., Rogaeva, E.A., St George-Hyslop, P.H., 1994. The upstream promoter of the beta-amyloid precursor protein gene (APP) shows differential patterns of methylation in human brain. Genomics 22, 340–347.
Sayre, L.M., Zelasko, D.A., Harris, P.L., Perry, G., Salomon, R.G., Smith, M.A., 1997. 4-hydroxynonenalderived advanced lipid peroxidation end products are increased in Alzheimer's disease. J. Neurochem. 68, 2092–2097.
Scarpa, S., Cavallaro, R.A., D'Anselmi, F., Fuso, A., 2006. Gene silencing through methylation: an epigenetic intervention on Alzheimer disease. J. Alzheimers Dis. 9, 407–414.
Schuessel, K., Schafer, S., Bayer, T.A., Czech, C., Pradier, L., Müller-Spahn, F., Müller, W.E., Eckert, A., 2005. Impaired Cu/Zn-SOD activity contributes to increased oxidative damage in APP transgenic mice. Neurobiol. Dis. 18, 89–99.
Singal, R., Ginder, G.D., 1999. DNA methylation. Blood 93, 4059–4070.
Smith, C.D., Carney, J.M., Starke-Reed, P.E., Oliver, C.N., Stadtman, E.R., Floyd, R.A., Markesbery, W.R., 1991. Excess brain protein oxidation and enzyme dysfunction in normal aging and in Alzheimer disease. Proc. Natl. Acad. Sci. U. S. A. 88, 10540–10543.
Tamagno, E., Parola, M., Bardini, P., Piccini, A., Borghi, R., Guglielmotto, M., Santoro, G., Davit, A., Danni, O., Smith, M.A., Perry, G., Tabaton, M., 2005. Beta-site APP cleaving enzyme up-regulation induced by 4-hydroxynonenal is mediated by stress-activated protein kinases pathways. J. Neurochem. 92, 628–636.
Tate, P.H., Bird, A.P., 1993. Effects of DNA methylation on DNA-binding proteins and gene expression. Curr. Opin. Genet. Dev. 3, 226–231.
Thomson, S., Mahadevan, L.C., Clayton, A.L., 1999. MAP kinase-mediated signaling to nucleosomes and immediate-early gene induction. Cell. Dev. Biol. 10, 205–214.
Tohgi, H., Utsugisawa, K., Nagane, Y., Yoshimura, M., Genda, Y., Ukitsu, M., 1999. Reduction with age in methylcytosine in the promoter region -224 approximately -101 of the amyloid precursor protein gene in autopsy human cortex. Brain Res. Mol. Brain Res. 70, 288–292.
Tong, Y., Zhou, W., Fung, V., Christensen, M.A., Qing, H., Sun, X., Song, W., 2005. Oxidative stress potentiates BACE1 gene expression and Abeta generation. J. Neural. Transm. 112, 455–469.
Valinluck, V., Tsai, H.H., Rogstad, D.K., Burdzy, A., Bird, A., Sowers, L.C., 2004. Oxidative damage to methyl-CpG sequences inhibits the binding of the methyl-CpG binding domain (MBD) of methyl-CpG binding protein 2 (MeCP2). Nucleic Acids Res. 32, 4100–4108.
van den Hove, D.L., Chouliaras, L., Rutten, B.P., 2012. The role of 5-hydroxymethylcytosine in aging and Alzheimer's disease: current status and prospects for future studies. Curr. Alzheimer Res. 9, 545–549.
Werner, P., Cohen, G., 1991. Intramitochondrial formation of oxidized glutathione during the oxidation of benzylamine by monoamine oxidase. FEBS Lett. 280, 44–46.
West, R.L., Lee, J.M., Maroun, L.E., 1995. Hypomethylation of the amyloid precursor protein gene in the brain of an Alzheimer's disease patient. J. Mol. Neurosci. 6, 141–146.
Williams, K., Christensen, J., Pedersen, M.T., Johansen, J.V., Cloos, P.A., Rappsilber, J., Helin, K., 2011. ET1 and hydroxymethylcytosine in transcription and DNA methylation fidelity. Nature 19, 343–348.
Wu, C., 1997. Chromatin remodeling and the control of gene expression. J. Biol. Chem. 272, 28171–28174.
Wu, H., D'Alessio, A.C., Ito, S., Wang, Z., Cui, K., Zhao, K., Sun, Y.E., Zhang, Y., 2011. Genome-wide analysis of 5-hydroxymethylcytosine distribution reveals its dual function intranscriptional regulation in mouse embryonic stem cells. Genes 1, 679–684.
Zawia, N.H., Lahiri, D.K., Cardozo-Pelaez, F., 2009. Epigenetics, oxidative stress, and Alzheimer disease. Free Radic. Biol. Med. 46, 1241–1249.
Zhu, W.G., Srinivasan, K., Dai, Z., Duan, W., Druhan, L.J., Ding, H., Yee, L., Villalona-Calero, M.A., Plass, C., Otterson, G.A., 2003. Methylation of adjacent CpG sites affects Sp1/Sp3 binding and activity in the p21(Cip1) promoter. Mol. Cell. Biol. 23, 4056–4065.